Triorganotin Fluoride Structures: A Ligand Close-Packing Model with Predominantly Ionic Sn−F Bonds

Jens Beckmann,[a] Dagmar Horn,[a] Klaus Jurkschat,*[a] Fred Rosche,[a] Markus Schürmann,[a] Uwe Zachwieja,[a] Dainis Dakternieks,*[b] Andrew Duthie,[b] and Allan E. K. Lim[b]

Keywords: Ab initio calculations / Chain structures / Hypervalent compounds / Tin / Fluorides / X-ray diffraction

The synthesis and complete characterization by multinuclear NMR, infrared, and Mössbauer spectroscopy, by single crystal X-ray analysis, as well as by electrospray mass spectrometry of the new soluble triorganotin fluoride Me_2PhSnF (**1**) is reported. The crystal structure of **1** reveals a *rod-like* polymeric structure in the solid state. Solutions of **1** in apolar solvents, such as toluene, contain mixtures of interconvertible oligomers. Ab initio MO calculations on model compounds H_3SnF, $[H_3SnFSnH_3]^+$, and $[FH_3SnFSnH_3F]^-$ indicate that the Sn–F bonds are substantially ionic in character, and suggest open-chain species, rather than cyclic species. In donor solvents, such as pyridine, **1** forms complexes with the solvent, such as Me_2PhSnF·pyridine. The solid-state structure of $(Me_3SiCH_2)_3SnF$ (**2**) is reformulated as monomeric with a weak intermolecular Sn···F interaction that gives rise to a [4+1] coordination. The relative short Sn–Sn separation enables the fluorine atoms to oscillate (flip-flop) between two neighboring $(Me_3SiCH_2)_3Sn$– groups, which is expressed in the X-ray experiment by a dynamic disorder. Ab initio MO calculations on a model compound, $[H_3SnFSnH_3]^+$, suggest only a small energy barrier for the flip-flop motion.

Introduction

Organometallic fluorides have received considerable attention owing to their structural diversity, which is associated with the ambivalent nature of fluorine. Fluorine is both monovalent and an excellent donor.[1] As it is also the most electronegative element, fluorine typically forms very polar or ionic bonds with most main-group elements[2] and transition metals.[3]

Triorganotin fluorides, R_3SnF, have been known for many decades,[4,5] and the nature of the Sn−F bonds remains controversial. Owing to its high melting point and virtual insolubility in organic solvents, Okawara et al. originally proposed an ionic structure for Me_3SnF.[6] However, on the basis of an early X-ray structure and IR and Raman spectroscopy, the structure of Me_3SnF was reformulated as a polymeric arrangement consisting of planar trimethyltin groups bridged by fluorine atoms.[7] Despite the fact that disorder precluded a satisfactory refinement of the X-ray structure of Me_3SnF, the comparatively short Sn−F bond lengths (2.15, 2.45 Å) and the slightly bent Sn−F−Sn bond angle (141°) were interpreted in terms of a predominantly covalent Sn−F bond character.[8−10] A similar arrangement was observed in the X-ray structure of nBu_3SnF; however, disorder again prevented the complete refinement of this structure.[11] Due to their bent Sn−F−Sn linkages, Me_3SnF and nBu_3SnF were both classified as *zigzag* polymers (**I**).[12] In contrast, the structures of the polymeric triorganotin fluorides Ph_3SnF[13] and $(PhCH_2)_3SnF$[14] consist of symmetric Sn−F−Sn bridges with equal Sn−F bond lengths (2.15 Å and 2.16 Å), whereas $cHex_3SnF$[15] contains unsymmetric bridges (2.05/2.30 Å). The latter compounds reveal (almost) linear Sn−F−Sn linkages and hence, are classified as *rod-like* polymers (**II**).[12]

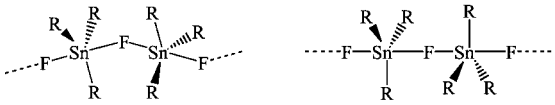

I **II**

The X-ray structure of $(Me_3SiCH_2)_3SnF$ deserves a special comment.[16] The authors suggested a *rod-like* polymer with symmetric Sn−F−Sn bridges. The two equally long Sn−F bonds (2.57 Å) were interpreted in terms of a highly ionic bond character.[15]

Monomeric structures have been reported for triorganotin fluorides containing more sterically demanding substitu-

[a] Fachbereich Chemie der Universität Dortmund, Lehrstuhl für Anorganische Chemie II,
44221 Dortmund, Germany
Fax: (internat.) + 49-(0)231/755-5048
E-mail: kjur@platon.chemie.uni-dortmund.de
[b] Centre for Chiral and Molecular Technologies, Deakin University,
Geelong, Vic. 3217, Australia
Fax: (internat.) + 61-0352/272218
E-mail: dainis@deakin.edu.au

ents, such as $[(Me_2PhSi)_3C]Me_2SnF$, $[(Me_3Si)_3C]Ph_2SnF$,[17] and $(2,4,6\text{-}Me_3C_6H_2)_3SnF$.[18] The latter compound was used to establish a standard "covalent" Sn−F bond length (1.96 Å).[18] Monomeric triorganotin fluorides were also obtained using the intramolecular coordination of the so-called *built-in* ligands.[19−23] Similarly, triorganotin fluorides react with additional fluoride ions to form monomeric triorganodifluorostannates, $R_3SnF_2^-$.[24−27]

Besides X-ray diffraction studies, ^{119}Sn Mössbauer spectroscopy,[12,28−41] ^{119}Sn MAS NMR spectroscopy,[42−47] IR spectroscopy,[6,10,36,48−52] and Raman spectroscopy[36,39,52] have been applied to distinguish between polymeric and monomeric triorganotin fluorides. Consequently, iBu$_3$SnF,[44] $(PhCH_2CH_2CH_2)_3SnF$,[53] and $(F_3C)_3SnF$[54] were assigned as polymeric structures, whereas $(PhMe_2CCH_2)_3SnF$,[53,55] $[(Me_3Si)_3C]Me_2SnF$,[17] $[(Me_3Si)(Me_2FSi)_2C]Me_2SnF$,[56] and $[(Me_3Si)_2(Me_2FSi)C]Me_2SnF$[57] have been identified as monomers. Furthermore, in the presumed polymeric triorganotin fluorides, R_3SnF (R = Me, Et, *n*Pr, *n*Bu, *n*Pen, *n*Hex, *n*Oct, *n*Dec), the effect of the lengths of the alkyl chain on the melting point, solubility, and the degree of crystallinity were studied, however, without the support of spectroscopy.[58]

Recently, Gillespie et al. used results from ab initio calculations to reinterpret the nature of bonds containing fluorine.[59] They concluded that a large majority of element−fluorine bonds, including Si−F bonds, possess substantial ionic character, and molecules such as SiF_4 are therefore more appropriately described using a ligand close-packing model with predominately ionic Si−F bonds.[60,61] A search of the literature revealed only two publications that included ab initio studies of molecules containing tin−fluorine bonds,[62,63] although neither of these studies focused directly on the nature of the Sn−F bonds.

The unusually high solubility of the new triorganotin fluoride $PhMe_2SnF$ enabled a comprehensive study of a polymeric triorganotin fluoride in solution. We now report on the results of this study, as well as on the reinvestigation of the structure of $(Me_3SiCH_2)_3SnF$.[16] The ab initio electronic structure calculations of the model compounds H_3SnF, $[H_3SnFSnH_3]^+$, and $[FH_3SnFSnH_3F]^-$ are also reported.

Results and Discussion

Dimethylphenyltin fluoride Me_2PhSnF (**1**) and tris(trimethylsilylmethyl)tin fluoride $(Me_3SiCH_2)_3SnF$ (**2**) were prepared in good yields from Me_2PhSnI and $(Me_3SiCH_2)_3SnCl$ (**2a**) by halide exchange reactions with KF and NH_4F, respectively, in a two-layer solvent system (water/diethyl ether) [Equation (1)].

$$R_2R'SnX \xrightarrow[-\ NH_4Cl\ or\ -\ KCl]{KF\ (ex)\ or\ NH_4F\ (ex)/H_2O/ether} R_2R'SnF \quad (1)$$

X = Cl, I

1, R = Me, R' = Ph

2, R = R' = CH_2SiMe_3

For putative polymeric triorganotin fluorides, **1** and **2** reveal very low melting points, 124−126 °C and 123−127 °C, respectively. In comparison, Me_3SnF and Ph_3SnF melt at temperatures exceeding 250 °C or decompose without melting.[4,5] This observation prompted us to investigate the structures of **1** and **2** in greater detail.

Characterization of 1 and 2 in the Solid State

The ^{119}Sn MAS NMR spectrum of Me_2PhSnF (**1**) exhibits a triplet centered at $\delta = -49.3$ ppm with a $^1J(^{119}Sn\text{-}^{19}F)$ coupling of 1235 Hz, thus unambiguously revealing a polymeric arrangement with symmetric Sn−F−Sn bridges on the NMR time scale. The ^{119}Sn MAS NMR parameters of **1** agree well with those reported for the polymeric parent compounds Me_3SnF [triplet at $\delta = 24.3$ ppm, $^1J(^{119}Sn\text{-}^{19}F) = 1300$ Hz] and Ph_3SnF [triplet at $\delta = -211.9$ ppm, $^1J(^{119}Sn\text{-}^{19}F) = 1530$ Hz].[44] The integration over all spinning sidebands of the three independent manifolds confirms the 1:2:1 ratio required for a triplet. The large sideband manifolds were also utilized to perform a tensor analysis according to the method of Herzfeld and Berger.[64,65] The isotropic chemical shielding (δ_{iso}), anisotropy (ζ), asymmetry (η) and chemical shift tensor components (σ_{11}, σ_{22}, σ_{33}) are presented in Table 1, alongside the same parameters for the related compounds Me_3SnF, Ph_3SnF, and $[Ph_3SnF_2]^-$.[27,44,45] Comparison of the data reveals that the average anisotropy for **1** is substantially larger ($|\zeta_{avg}| = 312$ ppm) than for Me_3SnF ($|\zeta_{avg}| = 221$ ppm), Ph_3SnF ($|\zeta_{avg}| = 250$ ppm) and $[Ph_3SnF_2]^-$ ($|\zeta_{avg}| = 219$ ppm), which clearly indicates that this parameter not only depends on the coordination number, but also on the local symmetry around the tin atoms. The lower symmetry in **1** as compared with Me_3SnF and Ph_3SnF is also reflected in the asymmetry, which is in the range between 0.80 and 1.00 for the three manifolds. For the parent compounds, which possess threefold symmetry axes, group theory requires the asymmetry to be 0.00,[66] which is indeed what was observed.[44,45]

In sharp contrast, the ^{119}Sn MAS NMR spectrum of $(Me_3SiCH_2)_3SnF$ (**2**) shows a doublet centered at 165.8 with a $^1J(^{119}Sn\text{-}^{19}F)$ coupling of 2167 Hz, indicating a monomer with tetracoordinated tin atoms. The ^{119}Sn MAS NMR parameters of **2** are similar to those of monomeric $(2,4,6\text{-}Me_3C_6H_2)_3SnF$ [two doublets due to crystallographically independent tin atoms at $\delta = -70.6$ ppm, $^1J(^{119}Sn\text{-}^{19}F) = 2300$ Hz; and $\delta = -82.2$ ppm, $^1J(^{119}Sn\text{-}^{19}F) = 2256$ Hz].[45] The integration over the two spinning sideband manifolds confirms that both sites of the doublet are of equal intensity. The reasonably small sideband manifolds of **2** were used to perform a tensor analysis as described above; the parameters obtained along with those for $(2,4,6\text{-}Me_3C_6H_2)_3SnF$ are presented in Table 1.[44] It is interesting to note that, for compound **2**, the asymmetry η is 0.00, which strongly indicates the presence of a threefold symmetry axis for the geometry around the tin atom;[66] this result is indeed confirmed by the single-crystal X-ray structure analysis (see below). The average anisotropy of **2** ($|\zeta_{avg}| = 95$ ppm) lies between those of the (symmetrically substituted) pentacoordi-

Table 1. Selected ^{119}Sn MAS NMR parameters for **1**, **2** and related compounds

Compound	δ_{iso}	ζ [ppm]	η	σ_{11} [ppm]	σ_{22} [ppm]	σ_{33} [ppm]
1	−39.3	−350.1	0.85	363	66	−311
	−48.2	−306.3	1.00	354	48	−258
	−57.0	+281.3	0.80	−196	29	338
Me_3SnF	41.5	−329	0.0	123	123	−370
	24.1	−221	0.0	87	87	−245
	6.7	−113	0.0	50	50	−120
Ph_3SnF	−198.1	−306	0.0	351	351	−108
	−211.9	−255	0.0	340	340	−43
	−225.2	−188	0.0	321	321	37
$[Ph_2SnF_2]^-$	−348.8	−276.5	0.20	515	459	72
	−362.7	−222.7	0.00	474	474	140
	−376.5	−158.0	0.20	471	440	218
2	154.7	154.7	0.00	−119	−119	−226
	169.4	169.4	0.00	−110	−110	−289
Mes_3SnF[a]						
(site 1)	−54.0	−51	0.2	85	74	3
	−84.8	75	0.1	42	53	160
(site 2)	−65.9	−62	0.3	107	87	3
	−96.0	63	0.3	55	74	159

[a] Mes = 2,4,6-$Me_3C_6H_2$.

nated compounds (Me_3SnF, Ph_3SnF, $[Ph_3SnF_2]^-$) and monomeric $(2,4,6\text{-}Me_3C_6H_2)_3SnF$ ($|\zeta_{avg}|$ = 63 ppm). Given that the symmetry of **2** is higher than that in $(2,4,6\text{-}Me_3C_6H_2)_3SnF$,[18] this observation may indicate a weak intermolecular Sn···F interaction ([4+1] coordination). Since this additional interaction is indeed confirmed by the single-crystal X-ray structure analysis (see below), it seems that the anisotropy ζ is more sensitive than the $^1J(^{119}Sn\text{-}^{19}F)$ coupling towards weak interactions. However, more systematic work is needed to prove this hypothesis.

The ^{119}Sn Mössbauer spectrum of **1** is also in good agreement with a polymeric structure.[37] The quadrupole splitting and the isomeric shift, 3.87 and 1.30 mm·s^{-1}, respectively, are indicative of pentacoordinated tin atoms. Notably, the quadrupole splitting and the isomeric shift for Me_3SnF and Ph_3SnF were reported to be 3.80 and 1.36 mm·s^{-1}, and 3.62 and 1.32 mm·s^{-1}, respectively.[36] In contrast, the Mössbauer spectrum of **2** is consistent with a monomeric structure containing tetracoordinated tin atoms; the quadrupole splitting and the isomeric shift are 2.97 and 1.29 mm·s^{-1}, respectively.[37]

In the pioneering work of Kriegsmann et al., the IR spectra of the triorganotin fluorides, R_3SnF (R = Me, Et, *n*Pr, *n*Bu), were compared, both in the solid state (polymeric) and in the gas phase (monomeric). They concluded that the asymmetric Sn−F stretching vibration for polymeric triorganotin fluoride compounds lies between 340 and 360 cm^{-1}, whereas for monomeric compounds the Sn−F stretching vibrations are between 530 and 590 cm^{-1}.[36,48,50] The IR spectrum (KBr pellet) of **1** shows a broad absorption at 340 cm^{-1}, consistent with a polymeric structure. In contrast, the IR spectrum (KBr pellet) of **2** shows no band between 300 and 400 cm^{-1}, but a band, which appears at 471 cm^{-1}, is tentatively assigned to an Sn−F stretching vibration. The position of this band lies between those of monomeric and polymeric triorganotin fluoride compounds. This supports the interpretation of the single-crystal X-ray diffraction analysis which shows that compound **2** exhibits a structure between the polymeric and monomeric forms, with a [4+1]-coordinated tin atom (see below).[36,48,50]

Single-Crystal X-ray Analyses of 1, 2, and 2a

The X-ray structure of Me_2PhSnF (**1**) is illustrated in Figure 1; selected bond parameters are collected in the caption of the figure, and details of the structure solution are listed in Table 3. Compound **1** features a slightly distorted *rod-like* polymeric arrangement with almost symmetric Sn−F bond lengths. All tin atoms in **1** are crystallographically related and adopt slightly distorted trigonal-bipyramidal geometries [geometrical goodness $\Delta\Sigma(\theta)$ = 88.4°], with the axial and equatorial positions occupied by two fluorine and three carbon atoms, respectively.[67,68] The slight distortion is best reflected in the C(1)−Sn(1)−C(11) and F(1)−Sn(1)−F(1a) bond angles, which are 116.5(1) and 179.44(7)°, respectively. The Sn−F bond lengths of **1** are 2.162(1) and 2.179(1) Å, and are only 0.016 and 0.033 Å longer than those of Ph_3SnF.[13] The tin atom is displaced by 0.030(2) Å from the plane defined by C(1), C(2), C(11), in the direction of F(1). In the crystal lattice, Me_2PhSnF (**1**) forms stapled layers of parallel but isolated polymer chains (Figure 2). The shortest distance between these polymer chains is 3.656(4) Å, between C(14) and C(16c) (c = 0.5 + x, y, −0.5 − z) of neighboring phenyl groups.

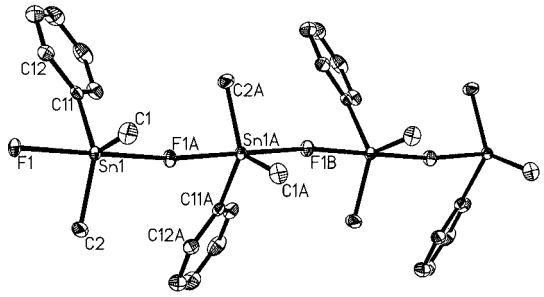

Figure 1. General view (SHELXTL) of a part of the polymeric chain of **1** showing 30% probability displacement ellipsoids and the atom numbering (SHELXTL-PLUS); selected bond lengths [Å] and angles [°]: Sn(1)−C(1) 2.112(3), Sn(1)−C(2) 2.115(3), Sn(1)−C(11) 2.123(3), Sn(1)−F(1) 2.162(1), Sn(1)−F(1a) 2.179(1), C(1)−Sn(1)−C(2) 121.7(1), C(1)−Sn(1)−C(11) 116.5(1), C(2)−Sn(1)−C(11) 121.7(1), C(1)−Sn(1)−F(1) 91.78(9), C(2)−Sn(1)−F(1) 89.99(8), C(11)−Sn(1)−F(1) 90.72(7), C(1)−Sn(1)−F(1a) 88.63(8), C(2)−Sn(1)−F(1a) 90.12(8), C(11)−Sn(1)−F(1a) 88.76(7), F(1)−Sn(1)−F(1a) 179.44(7), Sn(1)−F(1)−Sn(1b) 172.57(7) (symmetry transformation used to generate equivalent atoms: a = $-x$ + 1/2, y + 1/2, z; b = x, y − 1, z)

Despite having a very low melting point, Me_2PhSnF (**1**) is a polymer in the solid state. Apparently, this observation may simply be explained by the well-known correlation between the symmetry and the melting point of a molecule. It

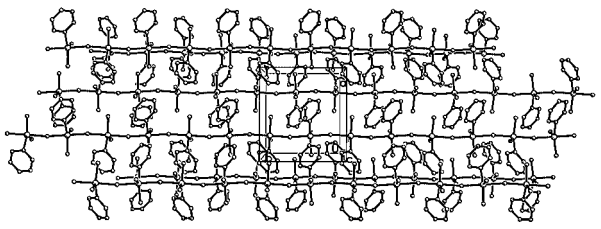

Figure 2. Perspective view (SHELXTL) of stapled layers of parallel polymer chains running through the crystal lattice of **1**

has been suggested that highly symmetrical molecules can absorb appreciable amounts of energy, before vibrations induce disruption from the crystal lattice.[69] In fact, all other structurally investigated polymeric triorganotin fluoride complexes bear three identical organic substituents and hence, possess a higher degree of symmetry than **1**.

The X-ray structure of $(Me_3SiCH_2)_3SnF$ (**2**) is illustrated in Figure 3; selected bond parameters are collected in the caption of the figure, and details of the structure solution are listed in Table 3. As previously reported by Zakharov et al.,[16] the structure of **2** is characterized by an infinite chain of tin atoms, with an Sn−Sn separation of 5.151(1) Å. However, the Sn−F distances are not equal [2.565(8) Å],[16] but show two pairs of different values [2.027(6)/3.125(6) Å and 2.377(6)/2.774(6) Å] as result of the dynamic disorder of the tin and fluorine atoms, respectively. The tin atoms exhibit strongly distorted trigonal-bipyramidal configurations [geometrical goodness $\Delta\Sigma(\theta)$ = 47.1° (Sn1), 54.0° (Sn1′)],[67,68] and represent positions halfway along the tetrahedron−trigonal bipyramid pathway. The distortion from the ideal trigonal bipyramid is reflected in the C−Sn(1)−C and C−Sn(1′)−C angles of 116.5(2) and 117.4(2)°, respectively. The origin for the deviation of these angles from tetrahedral is not mostly due to the steric hindrance of the organic substituents, as observed for Mes_3SnF (mean C−Sn−C 116.8°),[18] nor due to substituent electronegativity (Bent's rule),[70] but is rather the result of the intermolecular Sn(1)···F(1A) and Sn(1′)···F(1A) distances of 2.774(6) and 3.125(6) Å, respectively, being shorter than the sum of the van der Waals radii of tin and fluorine (3.63 Å).[70] This view is supported by the solid-state structure of $(Me_3SiCH_2)_3SnI$,[71] which shows C−Sn−C angles (111.7−115.2°) that are closer to those in a tetrahedral geometry.[72] Most interestingly, it appears that the intermolecular Sn···F interactions are not unambiguously reflected by the ^{119}Sn MAS NMR spectrum of **2**, which reveals a doublet and not a doublet of doublets (see above). The latter observation further strongly supports a dynamic rather than a statistical disorder in the structure of **2**. Given the sensitivity of ^{119}Sn MAS NMR spectroscopy, statistically disordered tin sites would give rise to the observation of two independent doublets. It is also worth mentioning that the molecular structure of $(Me_3SiCH_2)_3SnCl$ (**2a**) exhibits an analogous disorder, as shown in Figure 4; selected bond parameters are collected in the caption of the figure and details of the structure solution are listed in Table 2. The Sn−Sn separation in the infinite chain of tin atoms is 5.564(2) Å, and the pairs of Sn−Cl distances are 2.508(9)/3.056(9) and 2.498(10)/3.066(10) Å.[72] The geometrical goodness $\Delta\Sigma(\theta)$ of the respective tin atoms is 54.45° (Sn1) and 70.02° (Sn1′).[67,68]

Characterization of 1 and 2 in Solution

$PhMe_2SnF$ (**1**) and $(Me_3SiCH_2)_3SnF$ (**2**) are highly soluble in common organic solvents, such as chloroform, tolu-

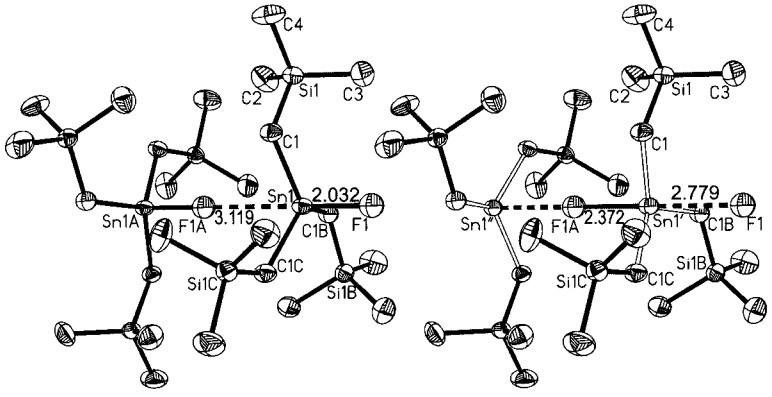

Figure 3. General view (SHELXTL) of **2** showing 30% probability displacement ellipsoids and the atom numbering scheme; selected bond lengths [Å] and angles [°]: disordered site 1: Sn(1)−C(1) 2.131(3), Sn(1)−F(1) 2.027(7), Sn(1)−F(1a) 3.125(7), C(1)−Sn(1)−C(1b) 116.5(2), C(1)−Sn(1)−F(1) 100.8(4), C(1)−Sn(1)−F(1a) 79.2(4), F(1)−Sn(1)−F(1a) 180.0; disordered site 2: Sn(1′)−C(1) 2.122(3), Sn(1′)−F(1) 2.774(6), Sn(1′)−F(1a) 2.377(6), C(1)−Sn(1′)−C(1b) 117.4(2), C(1)−Sn(1′)−F(1) 80.6(4), C(1)−Sn(1′)−F(1a) 99.4(4), F(1)−Sn(1′)−F(1a) 180.0 (symmetry transformations used to generate equivalent atoms: $a = -x, -y, z - 1/2$; $b = -y, x - y, z$; $c = -x + y, -x, z$)

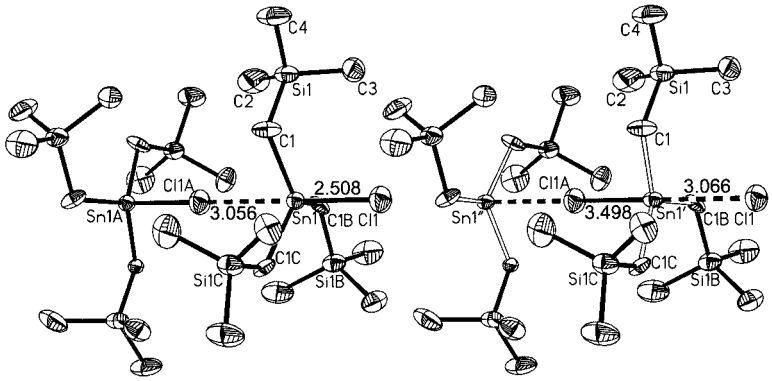

Figure 4. General view (SHELXTL) of **2a** showing 30% probability displacement ellipsoids and the atom numbering scheme; selected bond lengths [Å] and angles [°]: disordered site 1: Sn(1)−C(1) 2.154(4), Sn(1)−Cl(1) 2.508(9), Sn(1)−F(1a) 3.056(9), C(1)−Sn(1)−C(1b) 117.5(2), C(1)−Sn(1)−Cl(1) 99.3(3), C(1)−Sn(1)−Cl(1a) 80.7(3), Cl(1)−Sn(1)−Cl(1a) 180.0; disordered site 2: Sn(1′)−C(1) 2.136(3), Sn(1′)−Cl(1) 3.066(10), Sn(1′)−Cl(1a) 2.498(10), C(1)−Sn(1′)−C(1b) 119.0(1), C(1)−Sn(1′)−Cl(1) 94.3(3), C(1)−Sn(1′)−Cl(1a) 95.7(3), Cl(1)−Sn(1′)−Cl(1a) 180.0 (symmetry transformations used to generate equivalent atoms: $a = -x, -y, z - 1/2$; $b = -y, x - y, z$; $c = -x + y, -x, z$)

Table 2. Calculated NPA atomic charges for **3** and the staggered conformers of **4** and **5**

Molecule	$-q$(F) [au]	q(Sn) [au]	$-q$(H) [au]
3	0.723	1.545	0.274
4	0.743	1.522	0.217
5		1.607	0.302
bridging F	0.809		
terminal F	0.796		

ene, or methanol, which is in contrast to most polymeric triorganotin fluorides.[4,5]

The osmometric molecular weight determination of **1** (in toluene) reveals a strong, but steady concentration and temperature dependence, as illustrated in Figure 5. The highest molecular mass observed was 12000 g·mol^{-1}, corresponding to a degree of association exceeding 50 molecular units. In contrast, the molecular weight determination of **2** (in CH_2Cl_2) showed only the presence of monomers.5

Being consistent with the afore-mentioned ^{119}Sn MAS NMR spectrum, the ^{119}Sn NMR spectrum of **1** in [D$_8$]toluene displays a broad triplet at $\delta = -53.0$ ppm [$\nu_{1/2} = 250$, $^1J(^{119}\text{Sn-}^{19}\text{F}) = 1334$ Hz], the shape of which is somewhat distorted and similar to that reported for nBu$_3$SnF.[46] The ^{19}F NMR spectrum of **1** in [D$_8$]toluene shows a signal at $\delta = -139.0$ ppm ($\nu_{1/2} = 150$ Hz) with an unresolved $^1J(^{19}\text{F-}^{119/117}\text{Sn})$ coupling of 1260 Hz. Bearing in mind the natural abundance of the isotopes ^{119}Sn and ^{117}Sn, the magnitude of the integral ratio between the main signal and the tin satellites confirms the Sn−F−Sn connectivity. The presence of only one signal in both the ^{119}Sn and ^{19}F NMR spectrum suggests the fast exchange, on the ^{119}Sn and ^{19}F NMR time scales, of rapidly interconverting oligomers with varying degrees of association. We speculate that the $^1J(^{119}\text{Sn-}^{19}\text{F})$ coupling is maintained because the majority of F−Sn−F

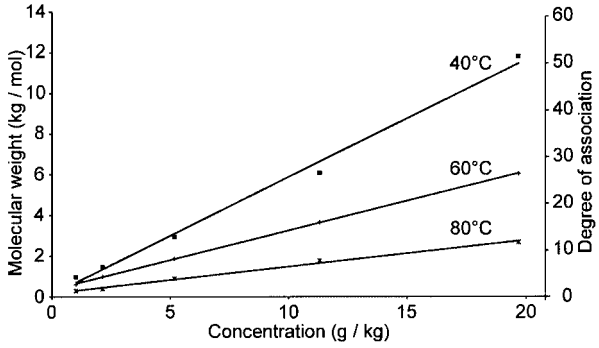

Figure 5. Osmometric molecular mass determination of **1** in toluene at 40, 60, and 80 °C (concentrations: 1.0, 2.1, 5.1, 11.3, 19.7 g·kg^{-1})

fragments present in these oligomers possess lifetimes that are comparatively long on the ^{119}Sn and ^{19}F NMR time scales.[46] Attempts to slow down the exchange process at −80 °C indeed show that the ^{119}Sn and ^{19}F spectra in [D$_8$]toluene become more complex. However, the broadness of the signals precluded the recognition of distinctive NMR multiplets or signals. All attempts to identify monomers at 80 °C or very low concentration (10 mg·mL^{-1} for ^{119}Sn; 0.25 mg·mL^{-1} for ^{19}F) failed. The IR spectrum of a saturated solution of **1** in CH_2Cl_2 shows a very strong asymmetric stretching Sn−F vibration at 339 cm^{-1}, which is almost identical to the corresponding band in the solid state and indicates bridging fluorine atoms.

At high molecular weights, a remarkable viscosity was noticed for solutions of **1** in toluene, which increases with higher concentrations and lower temperatures. Similar ob-

servations have already been reported for solutions of nBu$_3$SnF in different solvents, for which the effect was studied in greater detail.[73−75] Additives, such as pyridine or aniline, reduce the viscosity to that of the pure solvent.[73] No attempts were made to determine the viscosity of **1** in different solvents. Instead, a solution of **1** in [D$_5$]pyridine was investigated by ^{119}Sn NMR spectroscopy, which shows a broad signal centered at $\delta = -84.0$ ppm ($\nu_{1/2}$ = 800 Hz) at room temperature, and a doublet centered at $\delta = -91.5$ ppm ($\nu_{1/2}$ = 350 Hz) with a $^1J(^{119}\text{Sn-}^{19}\text{F})$ coupling of 1905 Hz at −25 °C. The ^{19}F NMR spectrum of the same solution at room temperature and at −25 °C shows a signal centered at $\delta = -168.6$ ppm [$^1J(^{19}\text{F-}^{119}\text{Sn}) = 1840$ Hz], and at $\delta = -164.4$ ppm [$^1J(^{19}\text{F-}^{119}\text{Sn}) = 2100$ Hz], respectively. The observation of a doublet in the ^{119}Sn NMR spectrum, and the intensity ratio of the satellites to the main signal in the ^{19}F NMR spectrum suggest the formation a monomeric complex, PhMe$_2$SnF·pyridine. An analogous complex, namely Ph$_3$SnF·pyridine, has already been mentioned in the literature.[24]

The ^{119}Sn NMR spectrum ($CDCl_3$) of **2** shows a doublet centered at $\delta = 193.0$ ppm with a $^1J(^{119}\text{Sn-}^{19}\text{F})$ coupling of 2340 Hz, which agrees reasonably well with the ^{119}Sn MAS NMR parameters (see above), although the difference in the chemical shift in solution and in the solid state (δ = 31.0 ppm) is much bigger than that in compound **1** (δ = 4.8 ppm). One possible explanation is that in solution the tetrahedral configuration of the tin atom in **2** is much less distorted than in the solid state, i.e. compound **2** is entirely monomeric. The ^{19}F NMR spectrum of **2** reveals a signal at $\delta = -207.2$ ppm, with a well-resolved $^1J(^{19}\text{F-}^{119}\text{Sn})$ coupling of 2370 Hz. The integration of the main signal with respect to the tin satellites confirms the monomeric structure.

Electrospray Mass Spectrometry

In order to identify the association of organotin ions with the parent compounds by autoionization, ESI MS spectra of PhMe$_2$SnF (**1**) and (Me$_3$SiCH$_2$)$_3$SnF (**2**) were recorded in acetonitrile. The following mass clusters showing the expected isotopic patterns were observed: **1**, negative mode: $Me_2PhSnF_2^-$ (265.0), $(Me_2PhSn)_2F_3^-$ (509.0), $(Me_2PhSn)_3F_4^-$ (753.0), positive mode: Me_2PhSn^+ (227.0), $(Me_2PhSn)_2F^+$ (471.0), $(Me_2PhSn)_3F_2^+$ (715.0), $(Me_2PhSn)_4F_3^+$ (961.0); **2**, negative mode: $(Me_3SiCH_2)_3SnF_2^-$ (419.1), positive mode: $(Me_3SiCH_2)_3Sn^+$ (381.1), $[(Me_3SiCH_2)_3Sn]_2F^+$ (779.2).

The ready formation of charged species suggests a highly ionic character of the Sn−F bonds in **1** and **2**. The degree of association is generally higher for species related to **1** than for those related to **2**, which correlates well with the observed Lewis acidities of the parent compounds. For some of the organotin anions detected under electrospray conditions, analogs were already identified in previous studies by ^{119}Sn NMR and ^{19}F NMR spectroscopy, e.g. $R_3SnF_2^-$ and $(R_3SnF)_2F^-$ (R = Me, nBu, Ph).[25,76,77] The observation of the uncoordinated (solvent-free) triorganotin cations, Me_2PhSn^+ (227.0) and $(Me_3SiCH_2)_3Sn^+$ (381.1), is also worth mentioning as the stabilities of such species were questioned for a long time.[78,79] Recently, the crystal structure of an isolated nBu$_3$Sn$^+$ cation (counter anion $CB_{11}Me_{12}^-$) undeniably proved the stabilities of these species.[80]

Conductivity measurements of **2** in acetonitrile, at $c = 10^{-3}$ mol·L^{-1}, reveal no change in conductivity compared with that of the pure solvent (1.7 μS). The result is consistent with extensive ion-pairing.

Ab Initio Computational Study of Model Compounds Containing Sn−F Bonds

The three model compounds H$_3$SnF (**3**), [H$_3$SnFSnH$_3$]$^+$ (**4**), and [FH$_3$SnFSnH$_3$F]$^-$ (**5**) were selected as subjects for the computational investigation. H$_3$SnF (**3**) is the simplest example of a monomeric tetravalent tin compound containing a tin−fluorine bond, whereas [H$_3$SnFSnH$_3$]$^+$ (**4**) and [FH$_3$SnFSnH$_3$F]$^-$ (**5**) represent two possible ways of defining a subsection of a polymeric tin fluoride chain. It is expected that the actual properties of the Sn−F−Sn linkages in a polymeric chain would be intermediate between those of the two extremes modeled herein. Furthermore, **4** and **5** resemble the corresponding ditin ions that have been detected in the ESI MS analyses of **1** and **2**.

The B3LYP/TZ-optimized structures of the model compounds, alongside selected geometric parameters are depicted in Figure 6. The calculated Sn−F bond length of H$_3$SnF (**3**) of 1.946 Å appears to agree with the Sn−F bond length of 1.961(4) Å observed in the monomeric triorganotin fluoride (2,4,6-Me$_3$C$_6$H$_2$)$_3$SnF.[18] For [H$_3$SnFSnH$_3$]$^+$ (**4**) and [FH$_3$SnFSnH$_3$F]$^-$ (**5**), staggered and eclipsed conformations were located on the potential energy surfaces; however, the differences in calculated bond lengths and angles between rotamers are negligible in both cases. Therefore, only the staggered conformations will be discussed here. As expected, the Sn−F distances increase when the coordination numbers of both tin and fluorine are increased: the Sn−F distance in **4** is 2.124 Å, and the distance from Sn to the bridging F atom in **5** increases further to 2.255 Å when the coordination number of tin is raised from four to five. This result is consistent with the experimentally obtained Sn−F bond lengths in polymeric organotin fluorides. For instance, the mean Sn−F bond lengths in **1**, Ph$_3$SnF, and cHex$_3$SnF are 2.171(2), 2.145(1), and 2.177(1) Å, respectively. The distance between the tin and the nonbridging fluorine atoms in **5** (2.041 Å) is also somewhat larger than the Sn−F distance in H$_3$SnF (**3**). The equilibrium Sn−F−Sn angles for all four fluorine-bridged ditin systems are calculated to be 180°. The SnH$_3$ moieties in **4** and **5** are effectively able to undergo free internal rotation, the calculated energy difference between the staggered and eclipsed conformations is only 0.02 kcal·mol^{-1} and 0.05 kcal·mol^{-1} for **4** and **5**, respectively. Both conformers of **4** and the staggered conformer of **5** are calculated to be minima on the B3LYP/TZ potential energy surface, whereas the eclipsed conformer of **5** is a first-order saddle point possessing one imaginary frequency (30i cm^{-1}) associated with rotation of the SnH$_3$ moieties towards the staggered con-

formation. The fact that the eclipsed conformer of **4** is calculated to be a minimum instead of a transition state analogous to the eclipsed conformer of **5**, could be an artifact due to the extreme flatness of the potential energy surface around the calculated stationary points, as illustrated by the very small difference in energy between the staggered and eclipsed conformations in **4**.

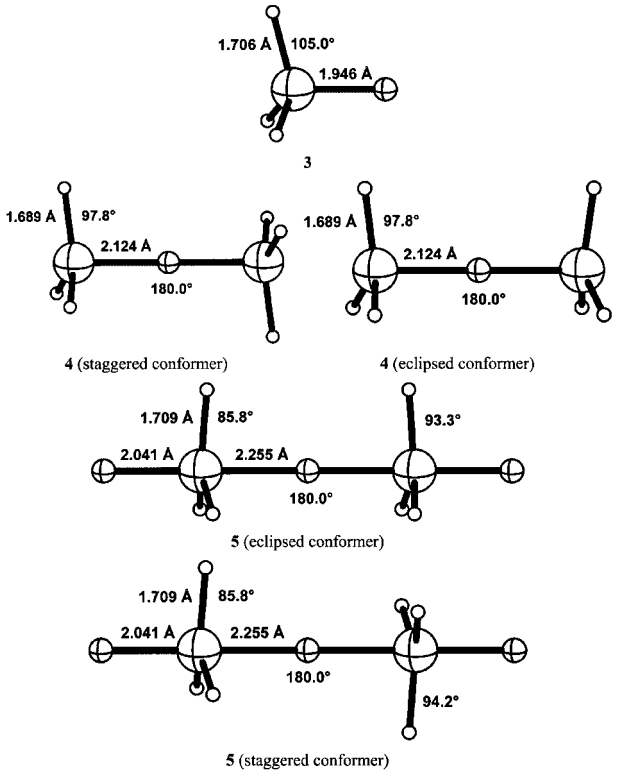

Figure 6. B3LYP/TZ-optimized structures and selected geometrical parameters of the model compounds **3**, and both eclipsed and staggered conformers of **4** and **5**

The Sn−F−Sn bending potential curves for both conformers of **4** and **5** are plotted in Figure 7. For both cases, it was found that the staggered conformation is slightly lower in energy than the eclipsed conformation at all Sn−F−Sn angles studied. The energy difference between the two conformers is smallest at the equilibrium Sn−F−Sn angle of 180°, and increases slightly as the Sn−F−Sn angle is reduced. This is consistent with the observation of staggered conformations in crystal structures of polymeric triorganotin fluorides, e.g. **1**, Ph_3SnF[13] and *c*Hex_3SnF.[15] However, the small energy differences calculated herein imply that the experimentally observed preference for polymeric triorganotin fluorides to adopt staggered conformations could be due to crystal-packing or steric effects, rather than electronic factors. All four curves are indicative of a very flat bending potential surface around the equilibrium Sn−F−Sn angle of 180°. Both curves corresponding to **4** lie below room temp. (= 0.6 kcal·mol^{-1}) between 160 and 180°, whereas the curves corresponding to **5** lie below room temp. between 140 and 180°. According to the criteria set forth by Gillespie et al., the linear Sn−F−Sn equilibrium angle and the high flexibility of the Sn−F−Sn linkages are indicative of highly ionic Sn−F bonds.[59] Thus, the observation of *zigzag* polymeric structures (bent Sn−F−Sn linkages) for Me_3SnF[8−10] and nBu_3SnF,[11] may be attributed to a combination of this flexibility and crystal packing effects, rather than being an indication of covalent bond character.[8−10] Despite the high flexibility of the Sn−F−Sn linkages, the preference of the F−Sn−F angles to be close to 180° (Bent's rule) precludes the formation of small or medium-sized rings in solution, e.g. similar to *cyclo*-$(R_2AlF)_3$.[81] The average internal angle of a *n*-membered ring is required by three-dimensional geometry to be less than (for puckered rings) or equal to (for flat rings) $[(n-2)/n] \times 180°$.[82] Constraining the F−Sn−F angles to be linear, would therefore necessitate large values of *n* before the Sn−F−Sn linkages are able to adopt favorable angles (> 150°).

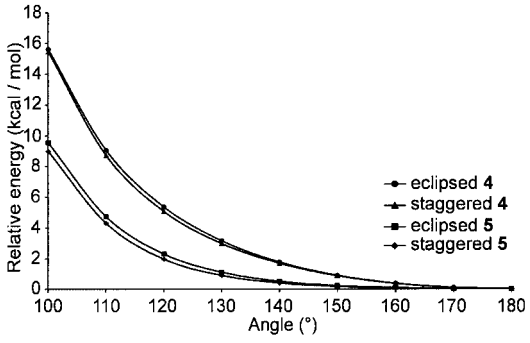

Figure 7. Energy profiles for the Sn−F−Sn bending deformations of both eclipsed and staggered conformers of **4** and **5**

Natural Population Analysis (NPA)[83] atomic charges calculated for **3** and the staggered conformers of **4** and **5** clearly show a significant localization of negative charge on the fluorine atoms in the model compounds, hence providing further evidence of the high ionic character of the Sn−F bond (Table 2). The bonds between tin and the bridging fluorine atoms are apparently slightly more ionic than the bonds between tin and non-bridging fluorine atoms.

In order to investigate the possibility that an oscillating (flip-flop) motion of the fluorine atoms between two neighboring tin atoms could be the reason for the disorder observed in the X-ray structure solution of **2**, a potential energy surface scan of the staggered conformer of **4** was performed, where the Sn−Sn separation is fixed at various values and the fluorine atom is moved from one tin atom to another. The calculated energy profiles are plotted in Figure 8. At a small Sn−Sn separation of 4.25 Å, which is extremely close to the equilibrium distance of 4.248 Å calculated for **4**, and a reasonable approximation to the measured Sn−Sn separations in the X-ray structures of all polymeric triorganotin fluorides, e.g. Ph_3SnF (4.29 Å),[13] $(PhCH_2)_3SnF$ (4.33 Å),[14] and **1** (4.33 Å), the curve re-

sembles a parabola with a minimum at the halfway point, where both Sn−F distances are 2.125 Å. However, when the Sn−Sn separation is increased, the curves become double-minimum potentials, which possess two minima approximately 2 Å away from the two tin atoms and a local maximum at the halfway point between the two tin atoms. This situation resembles that found in monomeric triorganotin fluorides, e.g. (2,4,6-$Me_3C_6H_2)_3SnF$ (Sn−Sn separation 6.42 Å, mean Sn−F distance 1.96 Å).[18] Most interestingly, the energy barrier between the two minima is found to increase substantially with increasing Sn−Sn separation. Thus, for very large Sn−Sn separations, as observed in (2,4,6-$Me_3C_6H_2)_3SnF$, the fluorine atoms are trapped in their respective potential wells. However, for reasonably small Sn−Sn separations, as observed in **2** (5.15 Å), the energy barrier is low enough to be exceeded and the fluorine atoms may oscillate (flip-flop) between the two potential wells. In the X-ray experiment of **2**, this motion is evidenced by a dynamic disorder (see above). It was further noticed that disorder prevented the complete refinement of the X-ray structure of Me_3SnF.[8−10] From the indisputable Sn−Sn separation (4.6 Å) it can be surmised that the disorder in Me_3SnF might also be due to dynamic factors rather than on statistical grounds.[84] In contrast, the Sn−Sn separation in the unsymmetric polymer *c*Hex_3SnF (4.35 Å)[15] is only marginally greater than in symmetric polymers, such as Ph_3SnF,[13] $(PhCH_2)_3SnF$,[14] and **1**. In view of the calculated energy profiles and the two unsymmetric Sn−F bonds (2.05/2.30 Å), the structure of *c*Hex_3SnF should also reveal a dynamic disorder reflected on the low energy barrier found for small Sn−Sn separations. In fact, the disorder of almost all carbon atoms in the structure of *c*Hex_3SnF strongly supports this assumption.[15]

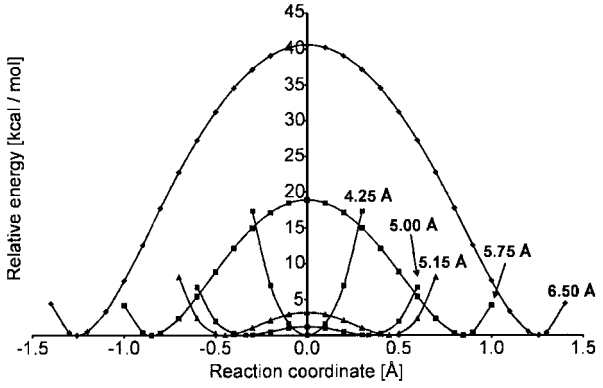

Figure 8. Energy profiles for the motion of the fluorine atoms from one tin atom to another in the staggered conformer of **4**, at Sn−Sn separations of 4.25, 5.0, 5.15, 5.75, and 6.5 Å; the zero of the reaction coordinate is set to the halfway point between the two tin atoms, where both Sn−F bond lengths are equal; calculated equilibrium Sn−F distances are 2.125, 2.165, 2.112, 2.026, and 1.992 Å, respectively

Experimental Section

General: ($Me_3SiCH_2)_3SnCl$ [$\delta(^{119}Sn)$ = 172.6 ppm] was prepared according to literature procedures.[85] Solution ^1H, ^{13}C, ^{19}F, ^{29}Si, and ^{119}Sn NMR spectra were obtained using a Bruker DRX 400 spectrometer. Chemical shifts (δ) are given in ppm and are referenced against $SiMe_4$, $SnMe_4$, and $CFCl_3$. ^{119}Sn MAS NMR spectra were recorded with a Bruker MSL 400 spectrometer using cross-polarization and high-power proton decoupling. An 8-μs 90° pulse, 5 ms of contact time and a recycle delay of 10 s were used. Chemical shifts (δ_{iso}) are quoted relative to $SnMe_4$, using solid *c*Hex_4Sn (δ_{iso} = −97.35 ppm) as a secondary reference. Typically, 12−15 K transitions were recorded for a signal-to-noise ratio suitable for tensor analyses. At least two experiments at independent spinning frequencies ranging from 4−12 kHz were recorded to determine the isotropic chemical shifts. The tensor analyses were performed according to the method developed by Herzfeld and Berger;[64][65] WINFIT software (Bruker) was used to analyze the spectra.[86] The principle components of the shielding tensors are reported using Haeberlen's notation as the isotropic chemical shift ($\delta_{iso} = -\sigma_{iso}$), the anisotropy ($\zeta = \sigma_{33} - \sigma_{iso}$) and the asymmetry ($\eta = |\sigma_{22} - \sigma_{11}|/|\sigma_{33} - \sigma_{iso}|$), σ_{11}, σ_{22}, σ_{33} are the three components of the shielding tensor expressed in its principal axis system with the following convention: $|\sigma_{33} - \sigma_{iso}| \geq |\sigma_{11} - \sigma_{iso}| \geq |\sigma_{22} - \sigma_{iso}|$.[87] With this convention, ζ is a signed value expressed in ppm and η is a dimensionless parameter, the value of which varies between 0 and 1. The Mössbauer spectra were recorded in constant-acceleration mode with a homemade instrument, designed and built by the Institut voor Kernen Stralingsfysica (IKS), Leuven, Belgium. The isomer shifts refer to a source of $Ca^{119m}SnO_3$ from Amersham, U.K., with the samples being maintained at 90(2) K. The data were treated with a least-squares iterative program that deconvoluted the spectrum into a sum of Lorentzians. FT infrared spectra were recorded using a Bruker IFS28 spectrometer. Electrospray mass spectra were obtained with a Platform II single quadrupole mass spectrometer (Micromass, Altrincham, U.K.) using an acetonitrile mobile phase. Acetonitrile solutions (0.1 mM) of the compounds were injected directly into the spectrometer via a Rheodyne injector equipped with a 50-μL loop. A Harvard 22 syringe pump delivered the solutions to the vaporization nozzle of the electrospray ion source at a flow rate of 10 $\mu L \cdot min^{-1}$. Nitrogen was used as both a drying gas and for nebulization with flow rates of approx. 200 $mL \cdot min^{-1}$ and 20 $mL \cdot min^{-1}$, respectively. Pressure in the mass analyzer region was usually about $4 \cdot 10^{-5}$ mbar. Typically 10 signal-averaged spectra were collected. Microanalyses were performed using an instrument from Carlo Erba Strumentazione (Model 1106). Molecular weight determinations were performed with a Gonotec Osmomat 070 osmometer.

Dimethylphenyltin Fluoride, Me_2PhSnF (1): A solution of PhMgBr (80 mL, 50.0 mmol) in THF, which was prepared from C_6H_5Br (7.85 g) and magnesium turnings (1.22 g), was added dropwise at 0 °C to a solution of Me_2SnCl_2 (5.00 g, 22.8 mmol) in THF (80 mL). The reaction mixture was heated at reflux for 1.5 h and the THF was distilled off. Diethyl ether (150 mL) was added to the residue and the resulting suspension was stirred for 15 min. This suspension was hydrolyzed with an aqueous HCl solution (50 mL, 4%), while cooling with ice. The organic layer was separated and the aqueous layer extracted three times with diethyl ether (30 mL). The combined organic phases were dried with Na_2SO_4. Filtration of the sodium sulfate and evaporation of the diethyl ether in vacuo gave Me_2Ph_2Sn (10.15 g, 33.5 mmol) as a yellow oil [$\delta^{119}Sn(CH_2Cl_2/D_2O$ capillary) = −60.1 ppm] of sufficient purity. Iodine (5.71 g, 45 mmol) was added in small portions to an ice-cooled magnetic-

ally stirred solution of Me_2Ph_2Sn (10.15 g, 22.5 mmol) in CH_2Cl_2 (100 mL). The reaction mixture was stirred at 0 °C for 2.5 h followed by the removal of dichloromethane and benzene in vacuo, giving a yellow oil, Me_2PhSnI (17.69 g) consisting of Me_2PhSnI [$\delta^{119}Sn(CH_2Cl_2/D_2O$ capillary) = −15.3 ppm]. A solution of KF (1.88 g, 32.4 mmol) in water (30 mL) was added to a solution of Me_2PhSnI (2.86 g, 8.1 mmol) in diethyl ether (30 mL). The reaction mixture was stirred for 24 h and was then left for a few hours without stirring giving rise to the formation of colorless crystals of Me_2PhSnF at the phase boundary (1.36 g, 6.7 mmol, 83% yield), m.p. 124−126 °C. ^1H NMR ($CDCl_3$): δ = 7.38 [complex pattern, $^2J(^1H\text{-}^{117/119}Sn)$ = 30 Hz, 2 H, *o*-H], 7.27 (complex pattern, 3 H, *m*-, *p*-H), 0.34 [s, $^2J(^1H\text{-}C\text{-}^{119/117}Sn)$ = 71 Hz, 6 H, *Me*] ppm. $^{13}C\{^1H\}$ NMR ($CDCl_3$, c = 0.228 mol·L^{-1}): δ = 144.6 [$^1J(^{13}C\text{-}^{117/119}Sn)$ = 707/741 Hz, C_i], 135.3 [$^2J(^{13}C\text{-}^{117/119}Sn)$ = 49 Hz, C_o], 128.6 (C_p), 127.9 [$^3J(^{13}C\text{-}^{117/119}Sn)$ = 65 Hz, C_m], −0.05 [$^1J(^{13}C\text{-}^{117/119}Sn)$ = 544/568 Hz, CH_3] ppm. ^{19}F NMR ($CDCl_3$): δ = −137.4 [$^1J(^{19}F\text{-}^{119/117}Sn)$ = 1255 Hz] ppm; ([D$_8$]toluene): δ = −139.0 [$^1J(^{19}F\text{-}^{119/117}Sn)$ = 1260 Hz] ppm. $^{119}Sn\{^1H\}$ NMR ($CDCl_3$): δ = −52.3 [$^1J(^{119}Sn\text{-}^{19}F)$ = 1340 Hz]; ([D$_8$]toluene): δ = −53.0 ppm [$^1J(^{119}Sn\text{-}^{19}F)$ = 1334 Hz] ppm. $^{13}C\{^1H\}$ MAS NMR: δ = −0.3, 1.6 (CH_3), 144.8, 136.6, 134.4, 128.5 (phenyl carbon atoms) ppm. $^{119}Sn\{^1H\}$ MAS NMR: δ = −49.5 [$^1J(^{119}Sn\text{-}^{19}F)$ = 1235 Hz] ppm. IR (KBr): $\tilde{\nu}$ = 3066 w, 2995 w, 2912 wbr, 1431 s, 1197 s, 1082 s, 998 w, 778 vs, 727 vs, 699 vs, 561 s, 531 s, 340 vs cm^{-1}. $C_8H_{11}FSn$ (244.91): calcd. C 39.2, H 4.5; found C 39.3, H 4.5.

Tris(trimethylsilylmethyl)tin Fluoride, $(Me_3SiCH_2)_3SnF$ (2): A saturated aqueous solution of NH_4F (30 mL) was added to a solution of $(Me_3SiCH_2)_3SnCl$ (0.80 g, 1.9 mmol) in diethyl ether (50 mL). The reaction mixture was stirred for 24 h and the organic layer was separated. The aqueous layer was extracted twice with diethyl ether (20 mL) and the combined organic phases were dried with Na_2SO_4. After filtration from the latter, the diethyl ether was distilled leaving a colorless residue which was recrystallized from dichloromethane giving $(Me_3SiCH_2)_3SnF$ (0.71 g, 1.8 mmol, 92% yield) of m.p. 123−127 °C. ^1H NMR ($CDCl_3$): δ = 0.11 (s, 27 H, CH_3), 0.23 [d, $^3J(^1H\text{-}^{19}F)$ = 4.2, $^2J(^1H\text{-}^{117/119}Sn)$ = 72.5/75.3 Hz, CH_2] ppm. $^{13}C\{^1H\}$ NMR ($CDCl_3$): δ = 6.1 [$^1J(^{13}C\text{-}^{119}Sn)$ = 286, $^2J(^{13}C\text{-}^{19}F)$ = 10 Hz; Sn*C*H$_2$Si], 1.5 (Si*Me*$_3$) ppm. ^{19}F NMR ($CDCl_3$): δ = −207.2 [$^1J(^{19}F\text{-}^{119}Sn)$ = 2369 Hz] ppm. $^{29}Si\{^1H\}$ NMR ($CDCl_3$): δ = 2.0 [$^2J(^{29}Si\text{-}^{119/117}Sn)$ = 29 Hz] ppm. $^{119}Sn\{^1H\}$ NMR ($CDCl_3$): δ = 196.4 [$^1J(^{119}Sn\text{-}^{19}F)$ = 2340, $^1J(^{119}Sn\text{-}^{13}C)$ = 282, $^2J(^{119}Sn\text{-}^{29}Si)$ = 30 Hz] ppm. $^{13}C\{^1H\}$ MAS NMR: δ = 3.7 (CH_3), 8.0 (broad, CH_2) ppm. $^{119}Sn\{^1H\}$ MAS NMR: δ = 165.8 [$^1J(^{119}Sn\text{-}^{19}F)$ = 2167 Hz] ppm. IR (KBr): $\tilde{\nu}$ = 2954 s, 2897 s, 1450 w, 1407 w, 1353 w, 1307 w, 1248 vs, 1023 vs, 833 vsbr, 752 s, 719 s, 689 s, 616 w, 596 s, 577 w, 529 s, 471 sbr, 283 w cm^{-1}. $C_{12}H_{33}FSi_3Sn$ (399.38): calcd. C 36.1, H 8.3; found C 36.2, H 8.1. Molecular weight (5.04 mg·g^{-1} CH_2Cl_2, T = 30 °C): 464 g·mol^{-1}.

X-ray Crystallographic Study: Intensity data for the colorless crystals were collected with a Nonius KappaCCD diffractometer with graphite-monochromated Mo-K_α radiation. The data collections covered almost the whole sphere of reciprocal space with 2 sets at different κ angles and 185 frames (**1**) and 360 frames via ω rotation (Δ/ω = 1°) (**2**, **2a**) at two times 5 s (**2a**), 10 s (**1**), and 30 s (**2**) per frame (Table 3). The crystal-to-detector distance was 3.0 cm (**2**, **2a**) and 3.4 cm (**1**). Crystal decay was monitored by repeating the initial frames at the end of the data collection. There was no indication for any decay when analyzing the duplicate reflections. The structure was solved by direct methods using SHELXS-97[88] and successive difference Fourier syntheses. Refinement was performed with full-matrix least-squares methods using SHELXL-97.[89] The

Table 3. Crystal data and structure refinement for **1**, **2**, and **2a**

	1	**2**	**2a**
Empirical formula	$C_8H_{11}FSn$	$C_{12}H_{33}FSi_3Sn$	$C_{12}H_{33}ClSi_3Sn$
Formula mass [g/mol]	244.86	399.34	415.79
Crystal system	orthorhombic	hexagonal	hexagonal
Crystal size [mm]	0.30 × 0.06 × 0.06	0.15 × 0.13 × 0.12	0.25 × 0.23 × 0.23
Space group	*Pbca*	*P*6(3)	*P*6(3)
a [Å]	9.3997(3)	10.6877(3)	10.6330(4)
b [Å]	8.6639(2)	10.6877(3)	10.6330(4)
c [Å]	22.3783(7)	10.3022(2)	11.1281(3)
V [Å^3]	1822.45(9)	1019.13(5)	1089.59(6)
Z	8	2	2
$\rho_{calcd.}$ [Mg/m^3]	1.785	1.301	1.267
T [K]	173(1)	291(1)	291(1)
μ [mm^{-1}]	2.748	1.423	1.446
F(000)	944	412	428
θ range [°]	3.68 to 27.48	2.96 to 24.98	3.83 to 25.02
Index ranges	$-12 \le h \le 12$ $-10 \le k \le 10$ $-29 \le l \le 29$	$-12 \le h \le 12$ $-10 \le k \le 10$ $-10 \le l \le 10$	$-12 \le h \le 12$ $-10 \le k \le 10$ $-11 \le l \le 11$
No. of reflections collected	10202	11175	12312
Completeness to θ_{max}	95.4%	93.8%	94.3%
No. of independent reflections/R_{int}	1998	1128	1226
No. of reflections observed with [$I > 2\sigma(I)$]	1246	820	833
No. of refined parameters	93	58	59
GooF (F^2)	1.014	0.912	0.940
$R1(F)$ [$I > 2\sigma(I)$]	0.0223	0.0228	0.0276
$wR2(F2)$ (all data)	0.0504	0.0538	0.0746
$(\Delta/\sigma)_{max}$	< 0.001	< 0.001	< 0.001
Largest difference peak/hole [e/Å^3]	0.793/−0.693	0.394/−0.182	0.376/−0.226

H atoms were placed in geometrically calculated positions using a riding model with U_{iso} constrained at 1.2 (for aryl groups) and 1.5 (for methyl groups) times U_{eq} of the carrier C atom. TWIN refinements were applied for **2** and **2a**, because a racemic twinning was present with a Flack parameter of 0.47(12) (**2**) and 0.52(13) (**2a**).[90] The TWIN refinement improved the *R* values of *R*1 [(0.0002) (**2**), (0.0003) (**2a**)] and of *wR*2 [(0.0004) (**2**), (0.0005) (**2a**)]. Atomic scattering factors for neutral atoms and real and imaginary dispersion terms were taken from International Tables for X-ray Crystallography.[91] The figures were created by SHELXTL.[92] CCDC-179688 (**1**), -179689 (**2**), and -179690 (**2a**) contain the supplementary crystallographic data for this paper. These data can be obtained free of charge at www.ccdc.cam.ac.uk/conts/retrieving.html or from the Cambridge Crystallographic Data Centre, 12 Union Road, Cambridge CB2 1EZ, UK [Fax: (internat.) + 44-1223/336-033; E-mail: deposit@ccdc.cam.ac.uk].

Acknowledgments

We thank the Deutsche Forschungsgemeinschaft, the Fonds der Chemischen Industrie and the Australian Research Council for financial support. The Australian National University Supercomputer Facility is acknowledged for a grant of supercomputer time. A. E. K. L. acknowledges an Overseas Postgraduate Research Scholarship from Deakin University. We acknowledge B. Mahieu (Louvain-la-Neuve, Belgium) for recording the Mössbauer spectra.

[1] H. W. Roesky, I. Haiduc, *J. Chem. Soc., Dalton Trans.* **1999**, 2249−2264.
[2] B. R. Jagirdar, E. F. Murphy, H. W. Roesky, *Prog. Inorg. Chem.* **1999**, *48*, 351−455.
[3] E. F. Murphy, H. W. Roesky, *Chem. Rev.* **1997**, *97*, 3425−3468.
[4] R. K. Ingham, S. D. Rosenberg, H. Gilman, *Chem. Rev.* **1960**, *60*, 459−539.
[5] *Gmelin Handbook of Inorganic Chemistry: Tin, Pt. 5: Organotin Fluorides, Triorganotin Chlorides*, Springer, Berlin, **1978**.
[6] R. Okawara, D. E. Webster, E. G. Rochow, *J. Am. Chem. Soc.* **1960**, *82*, 3287−3290.
[7] R. Okawara, M. Wada, *Adv. Organomet. Chem.* **1967**, *5*, 137−167.
[8] H. C. Clark, R. J. O′Brien, J. Trotter, *Proc. Chem. Soc.* **1964**, 85.
[9] H. C. Clark, R. J. O′Brien, J. Trotter, *J. Chem. Soc.* **1964**, 2332−2336.
[10] K. Yasuda, Y. Kawasaki, N. Kasai, T. Tanaka, *Bull. Chem. Soc. Jpn.* **1965**, *38*, 1216−1218.
[11] D. Williams, *Austr. Def. Stand. Lab., Annu. Rep.* **1967/8**, p. 37.
[12] K. C. Molloy, K. Quill, *J. Chem. Soc., Dalton Trans.* **1985**, 1417−1423.
[13] D. Tudela, E. Gutierrez-Puebla, A. Monge, *J. Chem. Soc., Dalton Trans.* **1992**, 1069−1071.
[14] H. Reuter, Ph.D. thesis, University of Bonn, **1986**.
[15] D. Tudela, R. Fernandez, V. K. Belsky, V. E. Zavodnik, *J. Chem. Soc., Dalton Trans.* **1996**, 2123−2126.
[16] L. N. Zakharov, Y. T. Struchkov, E. A. Kuz′min, B. I. Petrov, *Kristallografiya* **1983**, *28*, 271−275.
[17] S. S. Al-Juaid, S. M. Dhaher, C. Eaborn, P. B. Hitchcock, J. D. Smith, *J. Organomet. Chem.* **1987**, *325*, 117−127.
[18] H. Reuter, H. Puff, *J. Organomet. Chem.* **1989**, *379*, 223−234.
[19] M. Ochiai, S. Iwaki, T. Ukita, Y. Matsuura, M. Shiro, Y. Nagao, *J. Am. Chem. Soc.* **1988**, *110*, 4606−4610.
[20] U. Kolb, M. Dräger, B. Jousseaume, *Organometallics* **1991**, *10*, 2737−2742.
[21] U. Kolb, M. Dräger, M. Dargatz, K. Jurkschat, *Organometallics* **1995**, *14*, 2827−2834.
[22] I. Wharf, A. M. Lebuis, G. A. Roper, *Inorg. Chim. Acta* **1999**, *294*, 224−231.
[23] D. Dakternieks, K. Dunn, B. R. Vincent, E. R. T. Tiekink, *Main Group Met. Chem.* **2000**, *23*, 327−328.
[24] A. C. Sau, L. A. Carpino, R. R. Holmes, *J. Organomet. Chem.* **1980**, *197*, 181−197.
[25] S. J. Blunden, R. Hill, *J. Organomet. Chem.* **1989**, *371*, 145−154.
[26] M. Gingras, *Tetrahedron Lett.* **1991**, *32*, 7381−7384.
[27] J. Beckmann, D. Dakternieks, A. Duthie, E. R. T. Tiekink, *J. Organomet. Chem.*, **2002**, *648*, 204−208.
[28] R. V. Parish, R. H. Platt, *J. Chem. Soc., Chem. Commun.* **1968**, 1118−1120.
[29] R. V. Parish, R. H. Platt, *J. Chem. Soc. A* **1969**, *14*, 2145−2150.
[30] H. A. Stoeckler, H. Sano, *J. Chem. Soc. D* **1969**, 954−955.
[31] J. Devooght, M. Gielen, S. Lejeune, *J. Organomet. Chem.* **1970**, *21*, 333−343.
[32] R. V. Parish, R. H. Platt, *Inorg. Chim. Acta* **1970**, *4*, 65−72.
[33] N. N. Greenwood, B. A. Goodman, *J. Chem. Soc. A* **1971**, 1862−1865.
[34] R. H. Herber, S. Chandra, *J. Chem. Phys.* **1971**, *54*, 1847−1851.
[35] R. H. Herber, *J. Chem. Phys.* **1971**, *54*, 3755−3760.
[36] K. Licht, H. Geissler, P. Köhler, K. Hottmann, H. Schnorr, H. Kriegsmann, *Z. Anorg. Allg. Chem.* **1971**, *385*, 271−288.
[37] R. H. Platt, A. G. Maddock, *J. Chem. Soc. A* **1971**, 1191−1195.
[38] R. C. Poller, J. N. R. Ruddick, *J. Organomet. Chem.* **1972**, *39*, 121−128.
[39] R. H. Herber, J. Fischer, Y. Hazony, *J. Chem. Phys.* **1973**, *58*, 5185−5187.
[40] H. Negita, R. Boku, M. Sugiya, S. Ichiba, *Bull. Chem. Soc. Jpn.* **1980**, *53*, 3021−3022.
[41] R. Barbieri, A. Silvestri, G. Ruisi, G. Alonzo, *Inorg. Chim. Acta* **1985**, *97*, 113−117.
[42] R. K. Harris, K. J. Packer, P. Reams, *Chem. Phys. Lett.* **1985**, *115*, 16−18.
[43] R. K. Harris, P. Reams, K. J. Packer, *J. Mol. Struct.* **1986**, *141*, 13−25.
[44] H. Bai, R. K. Harris, H. Reuter, *J. Organomet. Chem.* **1991**, *408*, 167−172.
[45] H. Bai, R. K. Harris, *J. Magn. Reson.* **1992**, *96*, 24−30.
[46] Y. W. Kim, A. Labouriau, C. M. Taylor, W. L. Earl, L. G. Werbelow, *J. Phys. Chem.* **1994**, *98*, 4919−4922.
[47] J. C. Cherryman, R. K. Harris, *J. Magn. Reson.* **1997**, *128*, 21−29.
[48] K. Licht, H. Geissler, P. Köhler, K. Müller, *Z. Chem.* **1971**, *11*, 272−273.
[49] J. R. May, W. R. McWhinnie, R. C. Poller, *Spectrochim. Acta Part A* **1971**, *27*, 969−974.
[50] K. Licht, P. Köhler, H. Kriegsmann, *Z. Anorg. Allg. Chem.* **1975**, *415*, 31−42.
[51] R. H. Herber, *Polyhedron* **1985**, *4*, 1969−1974.
[52] A. S. Sall, O. Sarr, L. Diop, *Spectrochim. Acta* **1992**, *48A*, 613−614.
[53] H. Zimmer, O. A. Homberg, M. D. Jayawant, *J. Org. Chem.* **1966**, *31*, 3857−3860.
[54] R. Eujen, U. Thurmann, *J. Organomet. Chem.* **1992**, *433*, 63−77.
[55] W. T. Reichle, *Inorg. Chem.* **1966**, *5*, 87−91.
[56] D. A. Antonov, C. Eaborn, J. D. Smith, P. B. Hitchcock, E. Molla, V. I. Rozenberg, W. A. Stancyk, A. Kowaleska, *J. Organomet. Chem.* **1996**, *521*, 109−112.
[57] S. S. Al-Juaid, M. Al-Rawi, C. Eaborn, P. B. Hitchcock, J. D. Smith, *J. Organomet. Chem.* **1998**, *564*, 215−226.
[58] D. K. Dandge, C. Taylor, J. P. Heller, *J. Polym. Sci., Part A: Polym. Chem.* **1989**, *27*, 1053−1063.
[59] E. A. Robinson, S. A. Johnson, T.-H. Tang, R. J. Gillespie, *Inorg. Chem.* **1997**, *36*, 3022−3030.
[60] E. A. Robinson, G. L. Heard, R. J. Gillespie, *J. Mol. Struct.* **1999**, *485/486*, 305−319.
[61] R. J. Gillespie, *Coord. Chem. Rev.* **2000**, *197*, 51−69.

[62] K. O. Christe, D. A. Dixon, D. McLemore, W. W. Wilson, J. A. Sheehy, J. A. Boatz, *J. Fluorine Chem.* **2000**, *101*, 151−153.
[63] M. Kaupp, B. Metz, H. Stoll, *Angew. Chem. Int. Ed.* **2000**, *39*, 4607−4609.
[64] J. Herzfeld, A. E. Berger, *J. Chem. Phys.* **1980**, *73*, 6021−6030.
[65] J. Herzfeld, X. Chen, in: *Encyclopedia of Nuclear Magnetic Resonance*, John Wiley & Sons, New York, **1996**, vol. 7, pp. 4362−4369.
[66] A. D. Buckingham, S. M. Malm, *Mol. Phys.* **1971**, *22*, 1127−1130.
[67] M. Dräger, *Z. Anorg. Allg. Chem.* **1976**, *423*, 53−66.
[68] U. Kolb, M. Beuter, M. Dräger, *Inorg. Chem.* **1994**, *33*, 4522−4530.
[69] J. Timmerman, *J. Chim. Phys.* **1938**, *35*, 331.
[70] J. E. Huheey, E. A. Keiter, R. L. Keiter, *Inorganic Chemistry − Principles of Structure and Reactivity*, 4th ed., Harper Collins College Publishers, New York, **1993**.
[71] L. N. Zakharov, B. I. Petrov, V. A. Lebedev, E. A. Kuz′min, N. V. Belov, *Kristallografiya* **1978**, *23*, 1049−1051.
[72] M. Beuter, U. Kolb, A. Zickgraf, E. Brau, M. Bletz, M. Dräger, *Polyhedron* **1997**, *16*, 4005−4015.
[73] P. Dunn, D. Oldfield, *J. Macromol. Sci., Chem.* **1970**, *4*, 1157−1168.
[74] A. P. Evans, *J. Appl. Polym. Sci.* **1974**, *18*, 1919−1925.
[75] D. K. Dandge, C. Taylor, J. P. Heller, K. V. Wilson, N. Brumley, *J. Macromol. Sci., Chem.* **1989**, *A26*, 1451−1464.
[76] D. Dakternieks, H. Zhu, *Inorg. Chim. Acta* **1992**, *196*, 19−25.
[77] M. Jang, A. F. Janzen, *J. Fluorine Chem.* **1994**, *66*, 129−135.
[78] J. B. Lambert, B. Kuhlmann, *J. Chem. Soc., Chem. Commun.* **1992**, 931−932.
[79] J. B. Lambert, S. M. Ciro, C. L. Stern, *J. Organomet. Chem.* **1995**, *499*, 49−55.
[80] I. Zharov, B. T. King, Z. Havlas, A. Pardi, J. Michl, *J. Am. Chem. Soc.* **2000**, *122*, 10253−10254.
[81] C. Schnitter, K. Klimek, H. W. Roesky, T. Albers, H.-G. Schmidt, C. Roepken, E. Parisini, *Organometallics* **1998**, *17*, 2249−2257.
[82] J. Beckmann, D. Dakternieks, A. E. K. Lim, K. F. Lim, K. Jurkschat, *Organometallics*, manuscript submitted.
[83] A. E. Reed, R. B. Weinstock, F. Weinhold, *J. Chem. Phys.* **1985**, *83*, 735−746.
[84] S. P. Ionov, G. V. Ionova, *Zh. Fiz. Khim.* **1972**, *46*, 845−850.
[85] O. A. Kruglaya, G. S. Kalinina, B. I. Petrov, N. S. Vyazankin, *J. Organomet. Chem.* **1972**, *46*, 51−58.
[86] A. Massiot, H. Thiele, A. Germanus, *Bruker Report* **1994**, *140*, 43.
[87] U. Haeberlen, *Advances in Magnetic Resonance, Suppl. 1: High Resolution NMR in Solids: Selective Averaging*, Academic Press, New York, **1976**.
[88] G. M. Sheldrick, *Acta Crystallogr., Sect. A* **1990**, *46*, 467−473.
[89] G. M. Sheldrick, University of Göttingen, **1997**.
[90] H. D. Flack, *Acta Crystallogr., Sect. A* **1983**, *39*, 876−881.
[91] *International Tables for Crystallography*, vol. C, Kluwer Academic Publishers, Dordrecht, **1992**.
[92] G. M. Sheldrick, *SHELXTL, Release 5.1, Software Reference Manual*, Bruker AXS, Inc., Madison, **1997**.
[93] M. J. Frisch, G. W. Trucks, H. B. Schlegel, G. E. Scuseria, M. A. Robb, J. R. Cheeseman, V. G. Zakrzewski, J. A. Montgomery, R. E. Stratmann, J. C. Burant, S. Dapprich, J. M. Millam, A. D. Daniels, K. N. Kudin, M. C. Strain, O. Farkas, J. Tomasi, V. Barone, M. Cossi, R. Cammi, B. Mennucci, C. Pomelli, C. Adamo, S. Clifford, J. Ochterski, G. A. Petersson, P. Y. Ayala, Q. Cui, K. Morokuma, D. K. Malick, A. D. Rabuck, K. Raghavachari, J. B. Foresman, J. Cioslowski, J. V. Ortiz, B. B. Stefanov, G. Liu, A. Liashenko, P. Piskorz, I. Komaromi, R. Gomperts, R. L. Martin, D. J. Fox, T. Keith, M. A. Al-Laham, C. Y. Peng, A. Nanayakkara, C. Gonzalez, M. Challacombe, P. M. W. Gill, B. G. Johnson, W. Chen, M. W. Wong, J. L. Andres, M. Head-Gordon, E. S. Replogle, J. A. Pople, *Gaussian 98 (Revision A.7)*, Gaussian, Inc., Pittsburgh, PA, **1998**..
[94] A. Bergner, M. Dolg, W. Kuechle, H. Stoll, H. Preuss, *Mol. Phys.* **1993**, *80*, 1431−1441.
[95] S. Huzinaga, *Gaussian Basis Sets for Molecular Calculations*, Elsevier, New York, **1984**.
[96] A. Höllwarth, M. Böhme, S. Dapprich, A. W. Ehlers, A. Gobbi, V. Jonas, K. F. Köhler, R. Stegmann, A. Veldkamp, G. Frenking, *Chem. Phys. Lett.* **1993**, *208*, 237−240.
[97] A. D. Becke, *J. Chem. Phys.* **1993**, *98*, 5648−5652.
[98] C. Lee, W. Yang, R. G. Parr, *Phys. Rev. B: Condens. Matter* **1988**, *37*, 785−789.

Received July 9, 2002
[I02373]